Review of Scientific Instruments ARTICLE scitation.org/journal/rsi

Sapphire dilatometer cell for measuring the thermal expansion of solids

Cite as: Rev. Sci. Instrum. 93, 063903 (2022); doi: 10.1063/5.0091377
Submitted: 14 March 2022 • Accepted: 16 May 2022 •
Published Online: 7 June 2022

J. J. Neumeier[a] and Genevieve A. Nelson

AFFILIATIONS

Physics Department, Montana State University, Bozeman, Montana 59717-3840, USA

[a]Author to whom correspondence should be addressed: neumeier@physics.montana.edu

ABSTRACT

Capacitive-based dilatometry is used to determine the thermal expansion of solid specimens over a broad temperature range and for the study of structural and thermodynamic phase transitions. It can detect length changes of 0.1 Å or better. Dilatometer cells have been constructed of metals, such as copper or silver, and non-metals, such as silicon and fused silica. Sapphire is a good candidate for the construction of a dilatometer cell. It has excellent thermal conductivity, a well-behaved thermal expansion of moderate magnitude, especially below ~60 K, and is readily available. The design, fabrication, and testing of a sapphire dilatometer cell are described herein.

I. INTRODUCTION

The thermal expansion coefficient is important for evaluating the properties of solids from an engineering standpoint. It is also a fundamental thermodynamic quantity and a key element in the equation of state (EOS) for a solid. Armed with the EOS, numerous other thermodynamic quantities can be calculated. Thermal expansion measurements are important for the study of thermodynamic phase transitions, including normal-superconductor, paramagnetic–ferromagnetic, and paramagnetic–antiferromagnetic transitions, and for investigating structural transitions. For such studies, typical specimen sizes range from ~1 mm to ~1 cm. Absolute resolution for detecting ~0.1 Å length changes of the specimen is desirable.[1] Among various techniques for measuring thermal expansion, capacitive-based detection stands out for its excellent resolution and ability to measure fairly small specimens.[2–4] Typically, capacitive-based thermal-expansion cells, also referred to as dilatometer cells, have been made of metals such as copper or silver.[5–11] They have also been fabricated from silicon and fused silica.[12–14] Sapphire (single-crystalline α-Al_2O_3) is a desirable material from which to fabricate a dilatometer cell. Its thermal conductivity is very good, making it well suited for measurements at cryogenic temperatures. It is also an electrical insulator, thereby allowing for easy electrical isolation of metalized surfaces. Furthermore, high-quality sapphire is readily available. An absolute capacitance dilatometer was constructed from sapphire principally for measuring the thermal expansion of sapphire.[15] Additionally, mention of a sapphire dilatometer cell was made in a monograph,[4] but it was described only as poorly performing. This communication is the first report of a versatile dilatometer cell constructed entirely of sapphire.

II. MOTIVATION

Sapphire is well-known to possess a high thermal conductivity.[16–20] Comparison of the thermal conductivities of copper[20,21] (vacuum annealed, 99.99%), fused silica,[22] and sapphire is shown in Fig. 1(a). At 300 K, the thermal conductivity κ of copper is about 16 times larger than sapphire's, but at 100 K, they are approximately equal. Below this temperature, κ of sapphire surpasses copper's until about 10 K. At 3.1 K, κ of copper is four times larger than sapphire's, and by 0.4 K it is 225 times larger. Compared to fused silica, κ for sapphire is 1 to 4 orders of magnitude larger over the entire temperature range. At 2.5 K, the lowest temperature plotted for fused silica, sapphire's thermal conductivity is about 450 times larger. Note that the sapphire data in the figure extend to 0.4 K. In our work with the fused-silica dilatometer cell,[13] the poor thermal conductivity has required precise control of the warming rate (±0.001 K/min) (data are typically acquired on warming). Rapid changes in that rate lead to anomalous features in the data. Naturally, this is aggravated by the

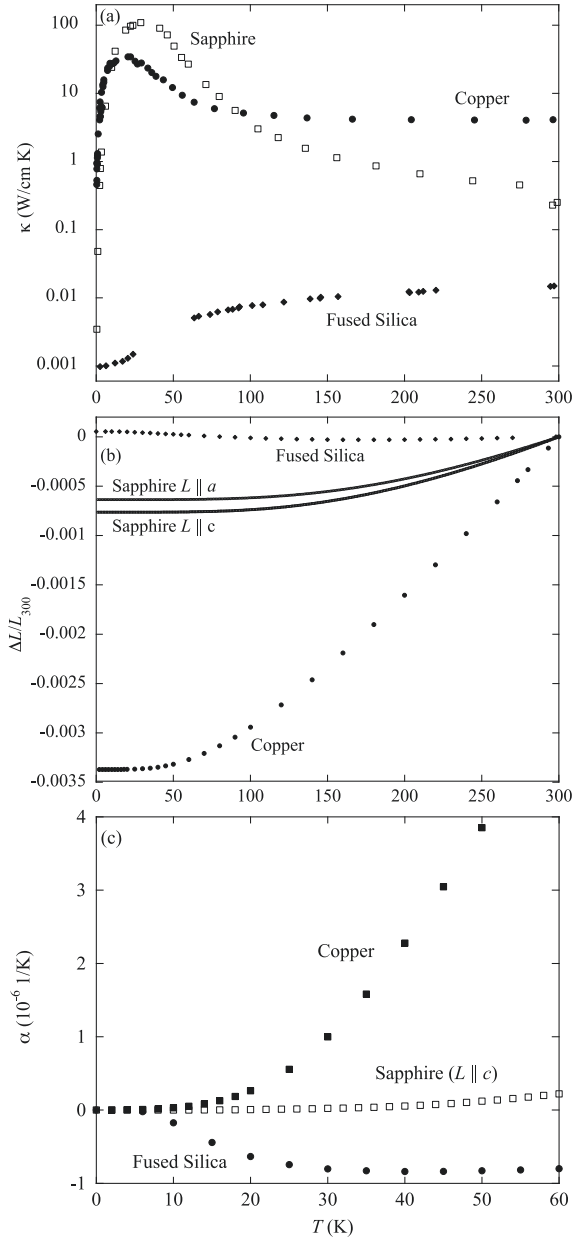

FIG. 1. Physical properties of sapphire, copper, and fused silica are plotted vs T for comparison. (a) Thermal conductivity κ vs temperature, (b) linear thermal expansion $\Delta L/L_{300}$, and (c) thermal expansion coefficient are shown.

fact that the measured changes in specimen length $\Delta L/L_{300}$ (L_{300} is the length at 300 K) are differentiated with respect to temperature T to yield the parameter of interest, the thermal expansion coefficient $\alpha = \mathrm{d}(\Delta L/L_{300})/\mathrm{d}T$. In principle, if the specimen and dilatometer cell can reach thermal equilibrium faster, the warming rate would become less critical. This could allow data to be acquired more rapidly and also allow more reliable measurement of features that exhibit hysteresis. These aspects were important motivations for this project.

Another important factor in choosing the material from which a dilatometer cell is constructed is the material's thermal expansion. This is due to two issues. The first is the empty-cell, or addenda, which must be subtracted from the raw data. The empty-cell effect can be understood upon considering the capacitance of a parallel-plate capacitor, $C = \varepsilon A/d$, where ε is the dielectric constant, A is the capacitor plate area, and d is the capacitor gap. If the cell material expands isotropically as a function of temperature, then $A(T) = A_{300}(1 + \Delta L/L_{300})^2$ and $d(T) = d_{300}(1 + \Delta L/L_{300})$. This leads to $C(T) = \varepsilon A_{300}(1 + \Delta L/L_{300})/d_{300}$. Thus, the smaller $|\Delta L/L_{300}|$, the smaller the empty-cell correction, other factors ignored. The second issue is that the measured capacitance change is due to the differential thermal expansion, i.e., the difference between the thermal expansion of the specimen and the cell.[6,13] Figure 2(a) illustrates the physical situation. The capacitor gap $d = L_S - (L_1 + L_2)$. Upon cooling imagine that L_S shrinks, making the capacitor gap *smaller*, but L_1 and L_2 also shrink, making the gap *bigger*. The data must be corrected for this differential expansion using the known thermal expansion of the material from which the cell is constructed. The smaller the thermal expansion of that material, the smaller the correction for differential expansion. Naturally, in order to accurately make these corrections, it is essential that the thermal expansion of the construction material is well known throughout the temperature range of use. Figure 1(b) displays the linear thermal expansion $\Delta L/L_{300}$ for sapphire measured along its a and c axes[4,23] (see Appendix A) compared to values for fused silica and copper. Clearly sapphire has a significantly smaller $|\Delta L/L_{300}|$ than copper, making it in this regard a better material for the construction of a dilatometer cell. While $|\Delta L/L_{300}|$ for fused silica seems the best choice when viewing Fig. 1(b), near 100 K the magnitudes of the thermal expansion coefficients α for fused silica and sapphire along c are comparable. Near 90 K their α magnitudes are at least 13 times smaller than copper. Figure 1(c) compares α for the three materials below 60 K.[24,25] Sapphire has the smallest $|\alpha|$ through most of the illustrated temperature range. This observation makes sapphire the best choice for measurements of the thermal expansion of solids below ~100 K, which was another important motivation for this project.

The construction of a dilatometer cell from a non-electrically conducting solid offers the advantage that the high and low capacitor plates are easily electrically isolated from one another. Dilatometer cells constructed from metals require the incorporation of insulating spacers to accomplish electrical isolation. The differential thermal expansions involved lead to features that must be subtracted from the raw data. Examples of such features for a copper cell based on a published design[10] are evidenced in a prior publication.[13]

Finally, a design was sought that would be small enough for use with the helium-3 refrigerator of the Quantum Design Physical Properties Measurement System (PPMS). The resulting cell would also need to be robust enough to be flipped upside down during the insertion of the refrigerator into the cryostat.

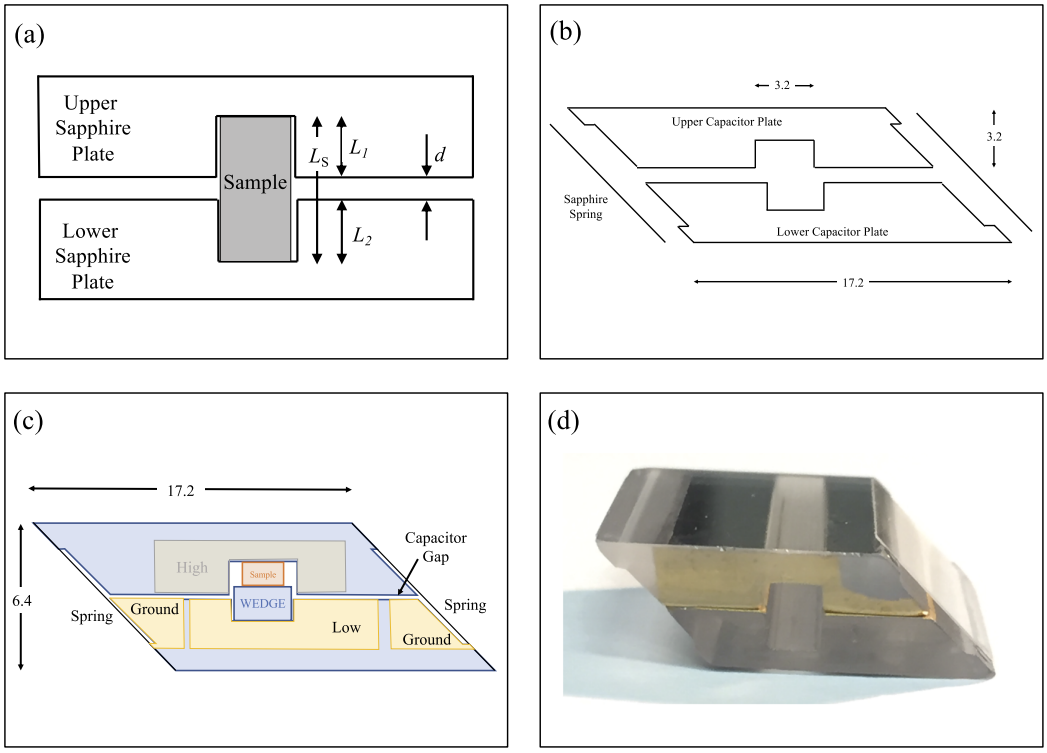

FIG. 2. (a) Schematic to clarify the differential expansion. No sapphire wedge is included, although it would not alter the differential expansion. (b) Schematic showing the five components of the cell. (c) Schematic of the assembled cell showing areas with metal deposition and an installed specimen and wedge. The high and low electrical terminals are on opposite sides of the cell. (d) Photograph of the finished cell before the addition of wiring. All lengths are in mm.

III. DESIGN AND FABRICATION

A. Design and construction of the main cell components

Two off-the-shelf *c*-axis oriented sapphire windows from Meller Optics, Inc. (Providence, RI USA), were used to fabricate the dilatometer cell. The windows were 25.4 mm in diameter and 3.2 mm thick. The sapphire windows were adhered to a ground-flat 6 mm thick magnetic steel plate with Crystalbond (Aremco Products, Inc., Valley Cottage, NY, USA), which was held fast with the magnetic chuck of a surface grinder. The surface grinder was fitted with 17.5 mm diameter resin-bonded diamond blades, 150 grit size (~100 μm), of required width, to grind the sapphire windows to the desired shape. Water was used as a coolant/lubricant during the grinding. To begin, two parallel cuts were made with a 1.4 mm wide blade, removing two circular edges of the windows, thereby reducing their widths to 19.6 mm. A magnetic steel block was milled with a 45° wedge on its top portion (see Appendix B). The wedge has a ledge to hold the sapphire workpieces at the required height. Both sapphire workpieces were adhered to the wedge using Crystalbond with their cut edges in contact with one another, both round edges in contact with the ledge. A 9 mm wide blade was used to simultaneously grind the round edge at the desired 45° angle at the required height. These ground edges are the surfaces to which the sapphire springs must be glued, however, only a narrow width is desired for the glue edge, otherwise, the spring's flexibility would be compromised. Therefore, additional grinding on these surfaces is required. Each surface received an indentation, leaving an elevated 1.8 mm wide lip to which the spring will be glued. Next, the two pieces are removed from the wedge, flipped 180°, shimmed to the appropriate height, adhered to the wedge with the less acute edge of the previously ground 45° resting on the ledge, and the last circular edges were ground flat at the desired 45° angle, creating a surface parallel to the angled surface of the opposing side. These surfaces then receive an indentation creating a 1.8 mm wide lip for the spring. Finally, channels are ground parallel to the capacitor plates for the specimen. A schematic illustrating the pieces for the cell is shown in Fig. 2(b). The channel on the upper plate is 3.2 mm wide at a depth of 1.5 mm parallel to the capacitor plate. The channel on the lower plate is ground with a similar depth but with a 3° angle along its length to accept a wedge with a corresponding 3° angle. Grinding at the 3° angle is accomplished by mounting the sapphire plate on a magnetic metal wedge with its upper surface at a 3° angle with respect to the magnetic chuck's surface. Sapphire wedges for mounting the

specimen in the cell were also ground using the same metal wedge. Multiple sapphire wedges with a variety of heights were prepared so that specimens with a range of lengths could be measured. Care must be taken when using the wedges that the *c*-axis of the wedge is parallel to the *c*-axis of the capacitor plate. Figure 2, panels (b) through (d), show schematic drawings of the cell parts and assembled cell to aid visualization.

Surfaces for the capacitor plates and electrodes were metalized using thermal vacuum deposition. All edges of the cell parts were rounded with sandpaper or diamond paper glued to the end of a wood popsicle stick, so that sharp, ragged edges did not develop into cracks and also to provide a rounded edge for the metal to be deposited on, thereby improving its durability. Areas of each sapphire part were masked with copper-beryllium sheets taking care to provide terminals for electrical contact and electrical continuity between the capacitor plate surfaces on opposing sides of the specimen channel on each plate. The electrical terminals for the high and low capacitor plates were placed on opposing sides of the cell to minimize the stray capacitance. Chromium was deposited first at a thickness of 155 Å followed by deposition of 1534 Å of copper. Using the tip of a phonograph stylus attached to an x–y stage, a separation was made to electrically isolate a guard ring from the low capacitor plate, about 1 mm from the edge. The guard ring helps to minimize fringe electric fields.[2,6] The resulting capacitor plate area is ~180 mm^2, almost identical to the plate area of the fused-silica cell[13] developed in our laboratory.

B. Springs

Thin sapphire plates with dimensions of 15 × 13 mm^2, 0.127(13) mm thick (*c*-axis perpendicular to the plate), were sourced from Guild Optical Associates, Inc. (Amherst, NH, USA) from their overstock items. Two were cut to dimensions of 15 × 8.9 mm^2. Once the cell was assembled (adhesive to be discussed below), an attempt was made to set a capacitor gap. Excessive force was needed to obtain a gap as compared to our experience with the fused-silica dilatometer cell developed in our laboratory. A few moments after setting the gap, one of the springs broke. Subsequently, we performed some testing by thinning scrap sapphire pieces of dimension 2.95 × 15.2× 0.127 mm^3 to the thickness of ~0.104 mm with a MTI UNIPOL-300 polishing machine using 45 μm diamond-coated paper. A bending test carried out by gripping 2 mm of the long axis while pushing down on the far end illustrated that repeated deflection of 1 mm was possible and breakage occurred at a deflection of 1.5 mm. Based on these observations, two new plates were selected and dimensioned. Since the force to bend a plate is proportional to the cross-sectional area, the spring size was narrowed to 13 mm, while the other dimension was reduced to 8.64 mm to better fit the cell. After cutting the plates to these dimensions, the freshly-cut edges were polished by hand with 45 μm and then 30 μm diamond paper, which was glued to the end of wood popsicle sticks. Their thicknesses were then reduced with the polishing machine. Diamond grits starting with 45 μm and finishing with 1 μm were used, resulting in a thickness of 0.111(3) mm. After polishing was complete, the springs were placed on a fused-silica block and annealed in air at 750° for 15 h to relieve stress. These springs provided good service, although professionally prepared springs with a thickness of 0.10 mm, with post-annealing, would be ideal.

C. Adhesive testing

Three adhesives and two surface preparation methods were evaluated. Sodium-silicate solution (three parts sodium silicate to one part H_2O), Krazy Glue, and Loctite Glass Glue were compared. The first preparation method consisted of chemical cleaning with acetone, methanol, and deionized (DI) water (denoted as *unprepared*), and the second added to this scrubbing with cerium oxide and DI water paste, rinsing with DI water, scrubbing with sodium bicarbonate and DI water paste, followed by a thorough rinse with DI water per the routine for hydroxide-catalysis bonding as described previously[26] (denoted as *prepared*). One specimen was tested using each type of glue and preparation method. Two pieces of sapphire were glued together, a weight was placed on top to promote strong bonding, and allowed to dry for several days. Specimens were then subjected to repeated thermal cycling from room temperature to 77 K in a liquid nitrogen bath and periodically checked for cracks or fissures in the bond. To test the strength of the bond, the specimens were periodically subjected to manual torsion, twisting the top and bottom bonded pieces in opposite directions by hand. Severe manual torsion was conducted following the completion of 35 thermal cycles to attempt to induce failure. The combination that survived the thermal cycling and manual torsion was found to be the prepared routine with sodium-silicate solution; the Loctite Glass Glue and Krazy Glue bonds failed under cycling (22 cycles and eight cycles, respectively).

Based on these results, sodium silicate solution was chosen as the bonding agent. The springs were cleaned ultrasonically in acetone (x2), methanol (x1), and DI water (x1). Finally, they were dried with nitrogen gas. After chemical cleaning, the *prepared* cleaning routine was applied. Surfaces were allowed to fully dry before gluing. The spring gluing surfaces of the upper and lower sapphire plates were also cleaned using the same steps, but manually with the cleaning agents applied via cotton swabs. The sapphire plates were placed on an aluminum gluing jig fitted with a magnet to hold the two capacitor plates in contact with each other when a magnet was placed on the outer edge of the cell (see Appendix B). Under a microscope, a spring was placed onto the spring surfaces. A small non-magnetic nut was then placed on top of the spring to keep the spring from becoming misaligned and to encourage a thin adhesive layer. Next, the spring was aligned such that the edge of the spring was flush with the bottom plate of the cell and centered on the spring mounting surfaces of the two capacitor plates. A thin wire taped to a rod, with a small loop in the wire's end is an effective tool for applying micro drops of glue. Sodium-silicate solution was applied to the joint; capillary action draws the solution across the glue joint. The glue should only be applied on the outer edges of the spring, otherwise, the springs can bend during drying. The glue joints for the first spring were allowed to dry overnight, then the cell was flipped over, and the second spring was glued in place.

Despite our adhesive testing, after 3 to 4 cooling cycles to 5 K in the measurement cryostat, the springs separated from the sapphire plates. This is probably due to absorption of water while the cell is in air after having been in the dry environment of the cryostat. Similar failures have been observed with our fused silica cell. Further adhesive testing is one avenue to address this. Another would be metallization of the springs and spring surfaces,

followed by soldering the springs in place, an approach used on a commercially-available dilatometer cell.[14]

IV. MEASUREMENT RESULTS

A. Experimental details

A simple, super-insulated bucket cryostat with a custom insert was used for the experiment.[13] The insert has a vacuum space separating the inner measurement chamber from the cryogenic bath. The inner stainless-steel tube of the measurement chamber has an high-purity copper can hard-soldered to its bottom in order to provide an isothermal region surrounding the cell. The can has a resistive heater on its outer diameter, which is used to warm the helium exchange gas surrounding the cell. A probe with a Faraday cage at its bottom holds the dilatometer cell. It has wiring for the capacitance measurement and thermometers. A shielded coax wire runs into the Faraday cage from the vacuum flange, and special attention is paid to all wiring to be certain that any stray capacitances are minimized (<10 aF). Platinum and Cernox thermometers are permanently mounted on the wall of the Faraday cage at the same vertical height as the specimen. After installation of the specimen in the cell and mounting of the cell in the probe, the probe is inserted into the measurement chamber, which is then evacuated. After pumping for ~1 h, the chamber is flushed with dry helium gas; this step is done twice before pumping for ~20 h while heating the dilatometer cell to a maximum temperature of 340 K to drive off residual moisture. Typically, a vacuum of $\sim 7 \times 10^{-6}$ mbar is attained. To enable thermal exchange, ~12 mbar of dry helium gas is admitted to the measurement chamber. The vacuum jacket is briefly pumped and 100 mbar of dry helium gas is admitted to that space. The capacitance is measured with an Andeen-Hagerling AH2500A ac capacitance bridge (1 kHz). The resistance of the thermometers is measured with a Lakeshore 340. The temperature is calculated from the resistances using a routine[13] in the LabVIEW data acquisition program. Typically, the dilatometer cell is cooled to about 5 K over the span of ~4 h. The LabVIEW program is then started, and the dilatometer cell is warmed at 0.200(1) K/min. Data are collected every 0.2 K. Additional details are available in Ref. 13.

B. Empty-cell measurement

In order to measure the empty-cell (addenda) effect, a sapphire wedge along with a small sapphire block near the cell's center was used to apply force to the upper capacitor plate, tension the springs, and establish a gap. Due to the anisotropy of sapphire, the capacitance should behave as

$$C(T) = \frac{\varepsilon A_{300}\left(1 + \Delta L^a/L^a_{300}\right)^2}{d_{300}\left(1 + \Delta L^c/L^c_{300}\right)}, \tag{1}$$

where $\Delta L^a/L^a_{300}$ and $\Delta L^c/L^c_{300}$ are the linear thermal expansions of sapphire along the a and c axes. Values of α for sapphire along a and c were obtained from Refs. 15 and 23 and integrated to yield the $\Delta L^a/L^a_{300}$ and $\Delta L^c/L^c_{300}$ values used in Eq. (1); see Appendix A for more details. The result is plotted in Fig. 3. The observed empty-cell effect is about 3.7 times larger in magnitude than the calculated effect, and it possesses a different temperature dependence. The change in capacitance shown in the measured empty-cell data corresponds to a change in the gap of 0.45 μm using the calibration factor found below. Thus, the effect is small, about equivalent to a wavelength of visible light. It can easily be subtracted from data acquired when measuring a specimen. Why the difference exists between the measured empty-cell effect, and the effect expected from Eq. (1) is difficult to say. Most likely it has to do with imperfect machining or assembly of parts, and the associated temperature variation thereof. In our experience with the fused-silica dilatometer cell, it is not uncommon to observe this level of disagreement with the calculated empty-cell effect.

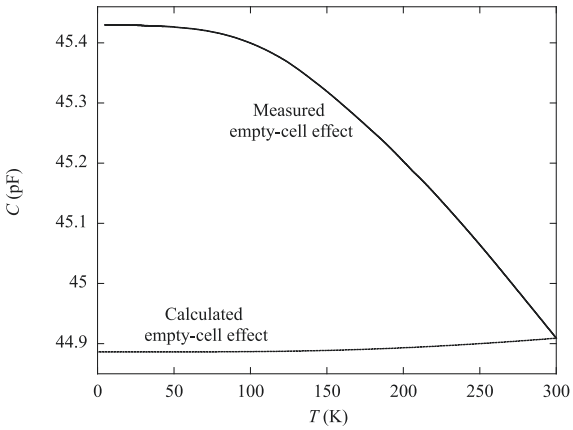

FIG. 3. Measured and calculated empty-cell effect for the sapphire dilatometer cell. The measured curve includes data acquired every 0.2 K from 5 to 300 K. The calculated curve was obtained with Eq. (1).

C. Calibration

The dilatometer cell was calibrated by measuring a specimen of high-purity copper with a length L_{Cu} = 1.948(1) mm. The specimen was installed on top of a sapphire wedge near the cell's center and pushed into the cell thereby lifting the upper plate to establish the gap at room temperature. The measurement followed the description in Sec. IV A. The measured empty-cell effect data were fitted with a cubic spline, which was used to generate values at the same temperatures as those of the copper measurement, which were then subtracted from the data. The corrected and raw data are shown in Fig. 4(a). The capacitor gap d was then calculated using an estimated value for εA (i.e., $d = \varepsilon A/C$), the data were corrected for the differential thermal expansion, and the obtained $\Delta L/L_{300}$ was calculated and compared to literature values.[24] The difference between $\Delta L/L_{300}$ and the literature values led to a new estimate for εA, leading to a new calculation of $\Delta L/L_{300}$. This process was iterated four times, ultimately yielding εA = 1775.8 μm pF and 0.003% agreement with the 6 K data point of Ref. 24. The discrepancies with the Kroeger and Swenson data[24] are +1.1% at 80 K, and +0.1% at 140 K, as a few examples. This is comparable to our fused-silica cell, where the discrepancy is generally no larger than 1%. We suspect that it can be attributed to the linear thermal expansion data for sapphire and/or copper used in the analysis.

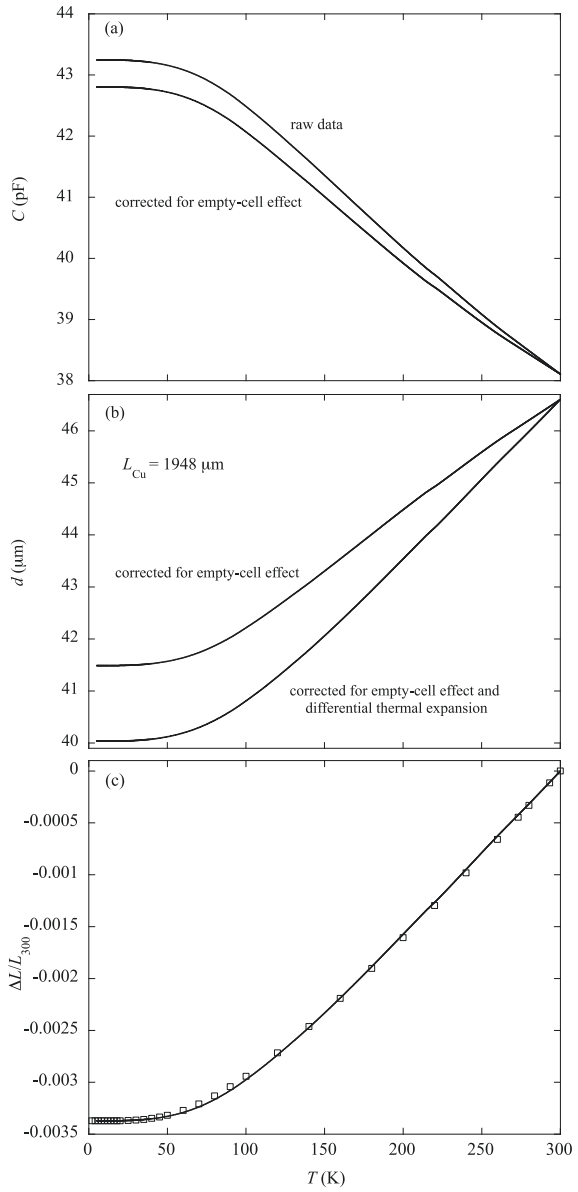

FIG. 4. (a) Raw capacitance data plotted vs temperature T for the measurement of the Cu calibration specimen L_{cu} = 1.948(1) mm. Data corrected for the empty-cell effect are shown. (b) Capacitor gap d vs T along with the gap after correction for the differential expansion of copper vs sapphire. (c) Resultant linear expansion of copper plotted along with the data from Ref. 24 (open symbols).

D. The normal-superconducting transition in MgB_2

At the normal-superconducting transition temperature T_c, a change in the slope of $\Delta L/L_{300}$ is expected, which leads to a jump in the thermal expansion coefficient α. This is often referred to as a second-order phase transition,[27] but more properly termed a continuous phase transition. Normally a continuous phase transition exhibits a λ-like shape, but it has been pointed out that such an anomaly could only be observed within a narrow region ($\Delta T/T_c \sim 10^{-3}$) near T_c in a superconductor.[28] Thus, only a jump in α is expected. Generally, this feature corresponds, over a 1 K temperature range near T_c, to a few Å change in specimen length. Thus, the normal-superconducting transition serves as a litmus test of a dilatometer cell's resolution. The superconductor measured here is MgB_2. The exact same specimen was measured previously with the fused-silica dilatometer cell, thereby allowing comparison with published results.[1]

Figure 5 panel (a) shows the capacitor gap d after subtraction of the empty-cell effect (lower curve) as described above. To correct for the differential expansion, the $\Delta L^c/L_0^c$ data for sapphire (see Appendix A) were fitted with a cubic spline, which was then used to generate values at the same temperatures as those of the MgB_2 data. The upper curve in Fig. 5(a) has been corrected for the differential expansion of the specimen and sapphire. The entire vertical range of Fig. 5(a) covers ~25 Å. This plot allows the reader to appreciate the relative magnitude of the correction along with the importance of having good values for the thermal expansion of sapphire. Panel (b) shows $\Delta L/L_5$ vs T. Note the vertical bar in the main panel representing a 2 Å change in specimen length. The inset focuses on the region below the transition with higher resolution; the vertical bar represents a 0.1 Å change in specimen length. Comparing the vertical bars to the scatter of the data, the resolution is sub-angstrom. The change in the slope of the data about either side of $T_c \sim 37.6$ K is due to the continuous normal-superconductor phase transition. Figure 5(c) shows the thermal expansion coefficient $\alpha = d(\Delta L/L_5)dT$, revealing the jump-like nature of the phase transition at T_c. These data were obtained via a point-by-point derivative. No smoothing of the data was done at any stage in the analysis. The vertical scatter of the data is largely associated with the resolution of the temperature channel, which has about 1000× poorer resolution than the capacitance channel.

While the jump in α shown at T_c in Fig. 5(c) reveals a magnitude that agrees extremely well with the published results,[1] the temperature dependence is quite different. In Ref. 1, α became negative immediately below T_c. Such a behavior is not observed here, and we believe this is because the correction for the differential expansion is much larger for the fused-silica cell used in that work, as indicated by the α values shown in Fig. 1(c). This observation illustrates a virtue of the sapphire dilatometer cell, due to the small, well-behaved thermal expansion of sapphire below 60 K, as discussed in Sec. II. Note the small bump in the data of Figs. 5(a) and 5(b) near 42 K. This is due to an increase in the warming rate from 0.20 to 0.57 K/m, associated with boil-off of all liquid helium from the cryostat. The small size of this feature compared to features observed under similar conditions with the fused-silica cell indicates that the large thermal conductivity of sapphire, over four orders of magnitude larger than fused silica's (and an order of magnitude larger than copper's) (see Fig. 1) in this temperature range, has improved the thermal equilibrium between the specimen, cell, and thermometer immensely. This underscores one of the virtues of sapphire as a material from which to construct a dilatometer cell, as discussed in Sec. II.

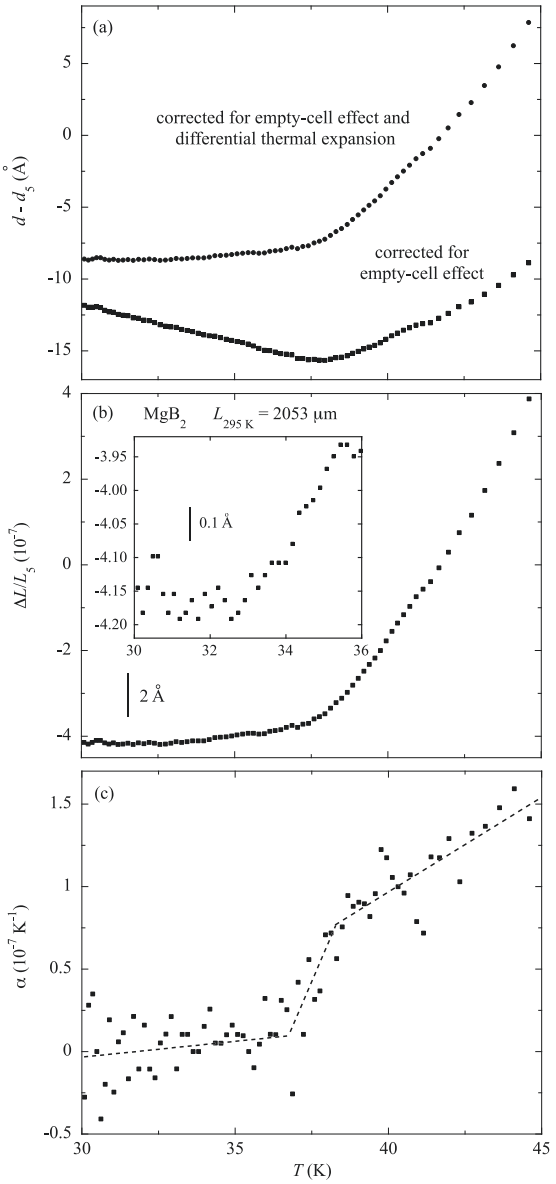

FIG. 5. Measurement data in the vicinity of the normal-superconducting phase transition T_c of a L_{295} = 2053(1) μm MgB_2 specimen. Panel (a) shows the capacitor gap d–d_5 plotted vs T (d_5 is the gap at 5 K). The lower curve has been corrected only for the empty-cell effect, and the upper curve has also been corrected for the differential expansion of the specimen and sapphire. (b) Linear thermal expansion of the specimen. The vertical bar, representing a 2 Å change in specimen length, is provided for reference. The change in slope about either side of T_c ~ 37.6 K is due to the continuous normal-superconductor phase transition. The inset focuses on the region below the transition, to illustrate the resolution of the device; the vertical bar represents a 0.1 Å change in specimen length. (c) Thermal expansion coefficient α calculated using a point-by-point derivative, illustrating the jump at the normal-superconducting phase transition T_c; dashed lines are guides. No smoothing was done in processing the data.

V. CONCLUSIONS

A dilatometer cell for measuring the thermal expansion of solids was constructed from sapphire. Sapphire has a number of advantages over other construction materials, including well-behaved thermal expansion and good thermal conductivity, and it is an electrical insulator. The low thermal expansion coefficient of sapphire makes the cell an especially good choice for measurements below ~60 K [see Fig. 1(a)]. The cell was calibrated using a copper standard. The data agree with published results on Cu within 1.1%. Measurements of the normal-superconducting phase transition of MgB_2 illustrate that it has the ability to resolve sub-angstrom changes of length and serve as a testament to some of the virtues of using sapphire for constructing a dilatometer cell. The cell's modest size makes it possible for use in constrained environments, such as the PPMS helium-3 refrigerator.

ACKNOWLEDGMENTS

This work was supported by the National Science Foundation Research Experience for Undergraduates Program through Grant No. PHY1950282. The authors thank Norman Williams for technical assistance.

AUTHOR DECLARATIONS

Conflict of Interest

The authors have no conflicts to disclose.

DATA AVAILABILITY

The data that support the findings of this study are available from the corresponding author upon reasonable request.

APPENDIX A: THERMAL EXPANSION VALUES FOR SAPPHIRE

Table I provides the thermal expansion values for sapphire used in this work. Values of α^c for the range 4.5 K $\leq T \leq$ 15 K were obtained from Ref. 15 via their fitting equation $\alpha(T) = 5.3(1.3)T^{2.9(0.15)} \times 10^{-13}$ K^{-1}. Values of α^a and α^c for the range 20 K $\leq T \leq$ 320 were obtained from the tabulated values of Ref. 23; the stated uncertainties are ~10^{-10} 1/K near 20 K, rising to <10^{-8} 1/K above 50 K. These combined datasets were fitted with a cubic spline, which had the constraint of being forced to pass through $T = \alpha = 0$ in accordance with the third law of thermodynamics. The cubic spline was then used to calculate α values at 1 K intervals, and then integrated to yield $\Delta L^a/L_0^a$ and $\Delta L^c/L_0^c$. Representative values from this fitting are provided in Table I. Extra digits beyond the measurement uncertainties reflect values obtained from the fit and are provided to aid readers in their own fittings and comparisons to future published values.

APPENDIX B: BLOCK FOR HOLDING SAPPHIRE PLATES AT 45° ANGLE AND GLUING JIG

Figure 6 shows a schematic of the magnetic steel block milled with a 45° angle on its top portion. The angled surface was stepped

TABLE I. Thermal expansion values for sapphire.

T (K)	α^a (10^{-6} 1/K)	α^c (10^{-6} 1/K)	$\Delta L^a/L_0^a$ (10^{-6})	$\Delta L^c/L_0^c$ (10^{-6})
0	0	0	0	0
2	⋯	1.2×10^{-5}	⋯	1.18×10^{-5}
4	⋯	3.8×10^{-5}	⋯	6.19×10^{-5}
6	⋯	11.4×10^{-5}	⋯	21.4×10^{-5}
8	⋯	24.4×10^{-5}	⋯	57.2×10^{-5}
10	⋯	44.0×10^{-5}	⋯	126×10^{-5}
14	⋯	11.3×10^{-4}	⋯	43.3×10^{-4}
16	⋯	22.6×10^{-4}	⋯	77.2×10^{-4}
20	31.9×10^{-4}	60.9×10^{-4}	31.9×10^{-4}	234×10^{-4}
30	0.0213	0.0222	0.154	0.158
40	0.0404	0.0545	0.463	0.520
50	0.0998	0.120	1.16	1.36
60	0.165	0.220	2.49	3.04
70	0.281	0.350	4.72	5.87
80	0.409	0.521	8.17	10.19
90	0.567	0.731	13.05	16.41
100	0.733	0.980	19.55	24.94
110	0.937	1.241	27.90	36.04
120	1.157	1.520	38.37	49.83
130	1.394	1.828	51.13	66.55
140	1.641	2.140	66.30	86.40
150	1.896	2.434	83.98	109.28
160	2.155	2.720	104.24	135.05
170	2.423	3.011	127.13	163.70
180	2.696	3.300	152.72	195.26
190	2.957	3.576	180.99	229.65
200	3.203	3.840	211.79	266.74
210	3.436	4.093	244.98	306.42
220	3.652	4.337	280.42	348.57
230	3.864	4.570	318.00	393.11
240	4.067	4.795	357.66	439.95
250	4.270	5.010	399.34	488.98
260	4.472	5.216	443.05	540.11
270	4.668	5.410	488.75	593.25
280	4.845	5.591	536.32	648.27
290	5.014	5.754	585.61	705.01
300	5.145	5.900	636.41	763.29
310	5.274	6.033	688.50	822.96
320	5.398	6.157	741.86	883.92

4.7 mm inward through the fabrication, providing a ledge to hold the sapphire workpieces at the required height as well as providing a parallel reference to the magnetic chuck's surface. Both sapphire workpieces were adhered to the steel block with their cut edges in contact with one another, both resting on the ledge. This block was used to grind the required 45° angles and to grind the indentations to these surfaces to provide ledges to which the springs would be adhered (see Fig. 2). An aluminum gluing jig similar to the design of this block, but only 38 mm in height, was also fabricated for holding the cell during gluing of the springs. Also with a 45° angle, when the two capacitor plates are placed in contact, and placed on the jig, the spring surface is horizontal. A slot was milled into the 45° aluminum surface to hold a permanent magnet with a width approximately equal to the dilatometer cell width. By placing a magnet on the outside of the outer sapphire plate, the two plates were held firmly together by the magnets, which forced the metalized surfaces into contact, making the capacitor plates parallel. The spring could then be glued in place.

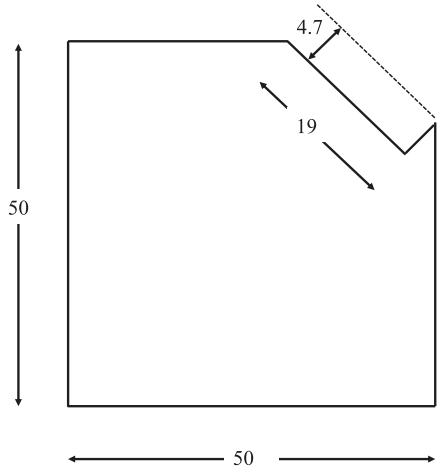

FIG. 6. Schematic diagram of the magnetic steel block used for grinding spring surfaces at the required 45° angle. Dimensions are in millimeters. The sapphire workpieces rest on the 4.7 mm ledge with their cut edges in contact, and their flat faces adhered to the surface inclined at 45°. The width of the block is 50 mm identical to the height and lengths are shown.

REFERENCES

[1] J. J. Neumeier, T. Tomita, M. Debessai, J. S. Schilling, P. W. Barnes, D. G. Hinks, and J. D. Jorgensen, "Negative thermal expansion of MgB_2 in the superconducting state and anomalous behavior of the bulk Grüneisen function," Phys. Rev. B **72**, 220505 (2005).

[2] G. K. White, "Measurements of thermal expansion at low temperatures," Cryogenics **1**, 151 (1961).

[3] B. Yates, "Thermal expansion," in *Monographs in Low-Temperature Physics*, edited by J. G. Daunt and K. Mendelssohn (Plenum Press, New York and London, 1972), Vol. 1.

[4] T. H. K. Barron and G. K. White, *Heat Capacity and Thermal Expansion at Low Temperatures* (Kluwer, New York, 1999) ISBN: 0-306-46198-6.

[5] G. Brändli and R. Griessen, "Two capacitance dilatometers," Cryogenics **13**, 299 (1973).

[6] R. Pott and R. Schefzyk, "Apparatus for measuring the thermal expansion of solids between 1.5 and 380 K," J. Phys. E: Sci. Instrum. **16**, 444 (1983).

[7] V. Horvatic, J. Gladic, Z. Vucic, and O. Milat, "An assessment of a new type of capacitance dilatometer for measurement of the thermal expansion of solids between 273 and 620 K," Meas. Sci. Technol. **2**, 381 (1991).

[8] M. Rotter, H. Müller, E. Gratz, M. Doerr, and M. Loewenhaupt, "A miniature capacitance dilatometer for thermal expansion and magnetostriction," Rev. Sci. Instrum. **69**, 2742 (1998).

[9] B. Kundys, Y. Bukhantsev, S. Vasiliev, D. Kundys, M. Berkowski, and V. P. Dyakonov, "Three terminal capacitance technique for magnetostriction and thermal expansion measurements," Rev. Sci. Instrum. **75**, 2192 (2004).

[10]G. M. Schmiedeshoff, A. W. Lounsbury, D. J. Luna, S. J. Tracy, A. J. Schramm, S. W. Tozer, V. F. Correa, S. T. Hannahs, T. P. Murphy, E. C. Palm, A. H. Lacerda, S. L. Bud'ko, P. C. Canfield, J. L. Smith, J. C. Lashley, and J. C. Cooley, "Versatile and compact capacitive dilatometer," Rev. Sci. Instrum. **77**, 123907 (2006).
[11]R. Küchler, T. Bauer, M. Brando, and F. Steglich, "A compact and miniaturized high resolution capacitance dilatometer for measuring thermal expansion and magnetostriction," Rev. Sci. Instrum. **83**, 095102 (2012).
[12]R. Villar, M. Hortal, and S. Vieira, "Silicon cell for the precise measurement of thermal expansion at low temperatures: Results for Cu and NaF," Rev. Sci. Instrum. **51**, 27 (1980).
[13]J. J. Neumeier, R. K. Bollinger, G. E. Timmins, C. R. Lane, R. D. Krogstad, and J. Macaluso, "Capacitive-based dilatometer cell constructed of fused quartz for measuring the thermal expansion of solids," Rev. Sci. Instrum. **79**, 033903 (2008).
[14]D. Martien, M. Williamsen, S. Spagna, R. Black, T. DaPron, T. Hogan, and D. Snow, "An ultrasensitive differential capacitive dilatometer," IEEE Trans. Magn. **55**, 6500204 (2019).
[15]V. B. Braginskii, S. I. Vasil'ev, and V. I. Panov, "Thermal expansion of aluminum oxide crystals at low temperatures," Sov. Tech. Phys. Lett. **6**, 287 (1980).
[16]R. Berman, E. L. Foster, and J. M. Ziman, "Thermal conduction in artificial sapphire crystals at low temperatures. I. Nearly perfect crystals," Proc. R. Soc. London, Ser. A **231**, 130 (1955).
[17]G. A. Slack, "Thermal conductivity of MgO, Al_2O_3, $MgAl_2O_4$, and Fe_3O_4 from 3 to 300 K," Phys. Rev. **126**, 427 (1962).
[18]M. W. Wolfmeyer and J. R. Dillinger, "Thermal conductivity of sapphire between 0.4 and 4 K," Phys. Lett. A **34**, 247–248 (1971).
[19]K. A. McCarthy and S. S. Ballard, "New data on the thermal conductivity of optical crystals," J. Opt. Soc. Am. **41**, 1062 (1951).
[20]G. E. Childs, L. J. Ericks, and R. L. Powell, "Thermal conductivity of solids at room temperature and below," *NBS Monograph* (National Bureau of Standards, Boulder, CO, 1973), Vol. 131.
[21]J. Nicol and T. P. Tseng, "Thermal conductivity of copper between 0.25 K and 4.2 K," Phys. Rev. **92**, 1062 (1953).
[22]D. H. Damon, "Thermal conductivity of vitreous silica at low temperatures," Phys. Rev. B **8**, 5860 (1973).
[23]G. K. White and R. B. Roberts, "Thermal expansion of reference materials: Tungsten and α-Al_2O_3," High Temp. - High Pressures **15**, 321 (1983).
[24]F. R. Kroeger and C. A. Swenson, "Absolute linear thermal expansion measurements on copper and aluminum from 5 to 320 K," J. Appl. Phys. **48**, 853 (1977).
[25]M. Okaji, N. Yamada, K. Nara, and H. Kato, "Laser interferometric dilatometer at low temperatures: Application to fused silica SRM 739," Cryogenics **35**, 887 (1995).
[26]R. Douglas, A. A. van Veggel, L. Cunningham, K. Haughian, J. Hough, and S. Rowan, "Cryogenic and room temperature strength of sapphire jointed by hydroxide-catalysis bonding," Classical Quantum Gravity **31**, 045001 (2014).
[27]A. B. Pippard, *The Elements of Classical Thermodynamics* (Cambridge University Press, London, 1961).
[28]V. L. Ginzburg, "Some remarks on phase transitions of the second kind and the microscopic theory of ferroelectric materials," Sov. Phys. Solid State **2**, 1824 (1961).